International Journal of Pharmaceutics 666 (2024) 124813

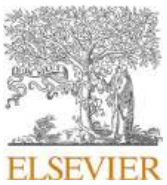

Contents lists available at ScienceDirect

International Journal of Pharmaceutics

journal homepage: www.elsevier.com/locate/ijpharm

Exploiting inhalable microparticles incorporating hybrid polymer-lipid nanoparticles loaded with Iloprost manages lung hyper-inflammation

Cinzia Scialabba, Emanuela F. Craparo *, Marta Cabibbo, Salvatore Emanuele Drago, Gennara Cavallaro

Lab of Biocompatible Polymers, Dpt of Biological, Chemical and Pharmaceutical Sciences and Technologies (STEBICEF), University of Palermo, Via Archirafi 32, Palermo 90123, Italy

ARTICLE INFO

Keywords:
Hybrid nanoparticles
Nano into micro
Iloprost
Hyper-inflammation
Cystic fibrosis
Pulmonary delivery

ABSTRACT

This study focuses on developing of a novel inhalation therapy for managing lung hyper-inflammation, producing hybrid polymer-lipid nanoparticles loaded with Iloprost (Ilo). These nanoparticles showed a size of approximately 100 nm with a core–shell structure and provided prolonged drug release, reaching 28 wt% after 6 h of incubation. The phospholipid composition and quantity (64 wt% on the total sample weight) result in minimal interaction with mucin and a significant effect on the rheology of a cystic fibrosis mucus model, in terms of reducing complex viscosity.

To obtain an inhalable microparticulate matrix suitable for incorporating Ilo@PEG-LPHNPs, the qualitative and quantitative composition of the feed fluid for the spray drying (SD) process was optimized. The selected composition (10 % wt/vol of mannitol and 10 % wt of ammonium bicarbonate relative to the weight of mannitol) was used to produce Nano-into Microparticles (NiM). The characterization of NiM revealed excellent aerodynamic properties, with a Mass Median Aerodynamic Diameter (MMAD) of 4.34 μm and a Fine Particle Fraction (FPF) of approximately 57 %. Biological characterization revealed that the particles are non-toxic to 16-HBE cells and can effectively evade macrophage uptake, likely due to the presence of PEG in their composition. Moreover, the delivered Iloprost significantly downregulates the production of the pro-inflammatory cytokine IL-6, showing the therapeutic potential of this drug delivery system.

1. Introduction

Recent advancements in drug formulation development aim to enhance pharmacotherapy by optimizing the use of existing medications on the market to further improve therapeutic efficacy (Etter et al., 2021). The main challenges in pharmaceutical technology involve enhancing the solubility and stability of drugs in biological fluids, as well as reducing the required dosage and frequency of administration. These goals are critical for minimizing potential adverse effects and improving patient compliance. In this context, nanomedicine has often proven to be a strategic and effective choice, not only in addressing these challenges but also in providing new opportunities for drug delivery (Neary et al., 2024; Pelaz et al., 2017).

A particular area of nanomedicine application is drug delivery to the lung, which holds great potential for the treatment of various respiratory disorders. Thanks to the development of innovative inhalable formulations, many drugs currently used in the treatment of pulmonary pathologies have been reassessed, providing advantages in terms of local bioavailability and reduction of undesired effects compared to the oral or parenteral drug administration (Gaikwad et al., 2023; He et al., 2019). Indeed, nanotechnology-based approaches allow to improve conventional inhaled therapies: nanoparticles can be engineered to encapsulate and protect drugs from degradation, release them in a controlled manner, and enhance their pulmonary retention. Furthermore, surface modifications of nanoparticles allow for specific targeting of diseased lung tissues, such as cancerous cells or inflamed airways.

In the field of drug delivery systems, polymeric nanoparticles and liposomes represent two dominant classes of nanocarriers capable of efficiently encapsulating and delivering a variety of drugs. Recently, hybrid polymer-lipid nanoparticles over all boast clear advantages, including high loading capacity and the possibility to carry both hydrophilic and hydrophobic drugs, better controlled release, biomimicry, and high biocompatibility, thanks to the fusion of features arising from colloidal nanostructured systems made solely of polymers or lipids

* Corresponding author.
E-mail address: emanuela.craparo@unipa.it (E.F. Craparo).

https://doi.org/10.1016/j.ijpharm.2024.124813
Received 26 July 2024; Received in revised form 18 September 2024; Accepted 6 October 2024
Available online 9 October 2024

(Khalili et al., 2022; Zhao et al., 2022). Moreover, the modulation of their surface characteristics can achieve precise release at the desired site, increase stability and safety in vivo, ultimately extend its half-life and enhance drug efficacy, which is a crucial aspect in supporting the use of a drug in therapy and could potentially facilitate its repositioning. In the case of hybrid nanostructured systems for local administration to the lung, the coating with endogenous and/or synthetic biomimetic phospholipids can reduce macrophage cell uptake, increasing the carrier's residence time at the site of action (Gonsalves and Menon, 2024).

Iloprost (Ilo), approved to treat pulmonary arterial hypertension (PAH) due to its potent vasodilatory action, has supplanted all prostacyclin analogues such as epoprostenol thanks to the commercialization of an inhalation formulation (Cipolla and Chan, 2018; Ewert et al., 2011; Gessler, 2019, 2018). The latter gives a reduction of Ilo systemic adverse effects, although to maintain therapeutic frequent inhalations are required due to Iloprost's short half-life of 3–5 min, which can lead to side effects such as cough and headache (Boucetta et al., 2024; Keshavarz et al., 2020). It's also worth noting that prostacyclin analogues can increase cAMP levels, and successfully enhance the expression and gating of the F508del-CFTR protein, as well as Ilo has demonstrated a potent pulmonary anti-inflammatory effect by the downregulation of pro-inflammatory cytokines, indicating it an excellent candidate for numerous conditions, including Cystic Fibrosis (CF) (Shaughnessy et al., 2022; Zhu et al., 2010). Therefore, there is a need for improvement of Ilo inhalation therapy, through the development of controlled – release formulations to avoid multiple dosing, intending to make it as easy and comfortable in lung disease treatment, optimizing its bioavailability and efficacy is even more useful and necessary to support its repositioning.

Recently, our research group developed an inhalation formulation based on microparticles incorporating Ilo-loaded polymeric nanoparticles to support an expansion of the therapeutic indications for the treatment of CF, by evaluating the drug's anti-inflammatory effect on CFBE cells overexpressing F508del CFTR mutation through the quantification of the expression of various pro-inflammatory cytokines (Craparo et al., 2024b).

Here, to modulate the drug release from the nanostructured carriers, optimize the administered dose and enhance their technological characteristics, and also improve the aerodynamic characteristics of the inhalable microparticles, we developed a more advanced and efficient formulation based on the Nano into Micro (NiM) strategy. This involved producing polymer-lipid hybrid nanoparticles as the nanostructured system to incorporate Ilo, offering improved performance compared to those previously reported in the literature (Craparo et al., 2024b). These systems were incorporated into a mannitol matrix, whose aerosolization performance was carefully optimized by using varying concentrations of mannitol and a porogen agent, a strategy already employed for other formulations proposed for inhalation (Chvatal et al., 2019; Craparo et al., 2024a). This approach aimed to improve deposition into the deep lung, dispersibility in pulmonary fluids, enhance cellular internalization, and controlled release profile.

The polymeric material chosen for the delivery of Ilo was the α,β-Poly(N-2-hydroxyethyl)-DL-aspartamide (PHEA), as its excellent properties as a drug colloidal carrier have already been demonstrated for the production of micelles (Triolo et al., 2017), gene delivery vectors (Perrone et al., 2021), and hybrid systems based on gold particles (Puleio et al., 2020).

2. Materials and Methods

2.1. Materials

Anhydrous N,N′-dimethylformamide (a-DMF), ammonium bicarbonate (AB), Rhodamine B (RhB), Acetonitrile for HPLC (ACN), methanol (MeOH), Poly(D,L-lactide-co-glycolide) (50/50) acid terminated (PLGA) (Mw = 7,000–17,000 Da), diethylamine (DEA), 1,1′-carbonyldiimidazole (CDI),ferric chloride hexahydrate ($FeCl_3$ $6H_2O$), ammonium thiocyanate (NH_4SCN), mucin from porcine stomach (type III, bound sialic acid 0.5–1.5 %), sodium chloride Dulbecco's phosphate buffer saline (DPBS), diethyl ether, dichloromethane, ethanol, 1,2-dipalmitoyl-*sn*-glycero-3-phosphocholine (DPPC), 1,2-distearoyl-*sn*-glycero-3-phosphoethanolamine-N-[methoxy (polyethylene glycol)-2000] (ammonium salt) (DSPE-PEG_{2000}) were purchased from Sigma-Aldrich (Milan, Italy). Endoprost was kindly provided by Italfarmaco. All reagents were of analytic grade unless otherwise stated. Dialysis membranes were purchased from Spectrum Labs (USA).

α,β-poly(N-2-hydroxyethyl)-DL-aspartamide (PHEA) and PHEA-g-RhB was prepared and purified according to the previously reported procedure (Craparo et al., 2022; Giammona et al., 2001).

The ^{1}H NMR spectra were recorded using Bruker Avance II 300 spectrometer operating at 300 MHz. Centrifugations were performed using a Coulter Allegra X-22R refrigerated centrifuge (Beckman).

2.2. Synthesis and characterization of PHEA-g-RhB-g-PLGA graft copolymer

The derivatization of PHEA-g-RhB with PLGA to produce the PHEA-g-RhB-g-PLGA graft copolymer was performed under an argon atmosphere, utilizing CDI as a coupling agent to activate the terminal carboxyl group of PLGA (Craparo et al., 2024a).

Initially, CDI was added to a solution of PLGA in anhydrous DMF at a concentration of 95 mg/mL, maintaining a ratio of 2 mmol CDI per mmol PLGA. This mixture was then stirred at 40 °C for 4 h to allow the CDI to activate the PLGA. Simultaneously, PHEA-g-RhB was dissolved in anhydrous DMF at a concentration of 33 mg/mL and maintained at 40 °C. DEA, acting as a catalyst, was added to this solution at a ratio of 5 mmol DEA per mmol PLGA.

Once the activation of PLGA was complete, the PHEA-g-RhB solution was added dropwise to the CDI-activated PLGA. This was done at a ratio of 0.05 mmol PLGA per mmol reactive units of PHEA. The combined reaction mixture was then stirred continuously at 40 °C for 48 h.

Following the reaction, the mixture was precipitated dropwise into diethyl ether. The resulting suspension was centrifuged at 4 °C for 15 min at a speed of 9800 rpm. The solid product obtained was washed several times with a mixture of diethyl ether and dichloromethane in a 45:55 vol ratio. After thorough washing, the solid was dried under vacuum and then weighed. The final product, PHEA-g-RhB-g-PLGA, was obtained with a yield of 45 % by weight based on the initial reagents and characterized as previously reported (Craparo et al., 2024a).

^{1}H NMR (300 MHz, d_7-DMF, 25 °C, TMS): δ 1.5–1.9 (m, 3H PLGA –[OCOCH($\mathbf{CH_3}$)]$_{92}$–); δ 2.8 (m, 2H PHEA –C(O)CH$\mathbf{CH_2}$C(O)NH–); δ 3.5 (t, 2H PHEA –NHC$\mathbf{H_2}$$CH_2$O–); δ 3.6 (t, 2H PHEA –NHCH_2C$\mathbf{H_2}$O–); δ 5.0 (m, 1H PHEA –NHC$\mathbf{H}$(CO)CH_2–); δ 4.2–4.5 and δ 5.4–5.8 (1H PLGA –[OCOC$\mathbf{H}$(CH_3)]$_{92}$–); δ 5.3 (2H PLGA –[OCOC$\mathbf{H_2}$]$_{92}$–).

The average molecular weight ($\overline{M}_w$) of PHEA-*g*-RhB-*g*-PLGA, determined by SEC analysis in organic phase, was found to be 130.5 kDa ($\overline{M}_w/\overline{M}_n$ = 1.2) (Craparo et al., 2024b).

2.3. Preparation of empty and Ilo-loaded polymeric nanoparticles

Empty and Ilo-loaded polymeric nanoparticles based on PHEA-g-RhB-g-PLGA graft copolymer (empty NPs and Ilo@NPs, respectively) were prepared by nanoprecipitation method (Craparo et al., 2024a). In detail, an organic copolymer solution was prepared by dissolving 75 mg of copolymer in 3.75 mL of acetone, containing or not 0.30 mg of Ilo (0.08 % w/v). The organic solution was then added dropwise under stirring to bidistilled water (1:10 v/v) and kept under stirring overnight. After that, the acetone was removed at 37 °C under reduced pressure, free Ilo was removed from the Ilo@NPs by centrifugation, and samples were stored at 5 °C for further analysis.

2.4. Preparation of Lipid − Polymer hybrid nanoparticles

Pegylated Lipid − Polymer Hybrid Nanoparticles (PEG-LPHNPs) were prepared by two step method involving the lipid vesicle preparation and the successive hybrid nanoparticles formation.

Lipid vesicles were prepared using the thin-layer evaporation method (TLE) (Craparo et al., 2022). A mixture of DPPC and DSPE-PEG_{2000} at a weight ratio of 3:1 was dissolved in chloroform. The organic solvent was then evaporated under vacuum at 40 °C, forming a lipid film, which was rehydrated with 10 mL of phosphate buffer at pH 7.4, achieving a final lipid concentration of 0.5 wt%. The mixture was stirred in a water bath at 75 °C for 30 min.

In the next step, empty and Iloprost-loaded lipid-polymer hybrid nanoparticles (referred to as PEG-LPHNPs and Ilo@PEG-LPHNPs, respectively) were prepared by mixing the aqueous dispersions of nanoparticles and the buffered dispersion of lipid vesicles at a polymer/lipid ratio of 2:5 (w/w). This physical mixture was then subjected to high-pressure homogenization (HPH) at a pressure of 10,000 to 15,000 psi using an EmulsiFlex-C5 homogenizer. The resulting dispersions were purified by ultracentrifugation and the resulting pellet was freeze-dried and stored for further characterization.

Moreover, un-pegylated samples (LPHNPs) were prepared as above, starting from DPPC − based lipid vesicles.

2.5. Characterization of Lipid − Polymer hybrid nanoparticles

2.5.1. Dimensional analysis and ζ-Potential measurements

The size distribution and polydispersity index (PDI) of each sample were evaluated by Dynamic light scattering measurement. The analysis was performed on water dispersion of each sample (1 mg/mL) using a Malvern Zetasizer NanoZS (Malvern Instruments, Worcestershire, U.K.) instrument equipped with a 632.8 nm laser with a fixed scattering angle of 173°. The same instrument was used for zeta potential measurement. Zeta potential values (mV) were calculated from electrophoretic mobility using the Smoluchowski relationship. Analyses were performed in triplicate.

2.5.2. Transmission electron microscopy (TEM)

Sample morphology was determined by transmission electron microscopy (TEM). Each sample was incubated on a 200 mesh formvar-coated grid (TAAB Ltd., Singapore) for 10 min at RT. After removing the excess of solution from the grid, samples were negatively stained with Uranyless (Electron Microscopy Sciences, Hatfield, PA, USA) for 5 min at RT and examined using TEM (Tecnai G2 Spirit; FEI Company, Eindhoven, The Netherlands) at 80 kW.

2.5.3. Phospholipid quantification

The lipid content in hybrid nanoparticles was quantified by Stewart's phospholipid colorimetric assay which forms a complex between the phospholipid and ammonium ferrothiocyanate (Craparo et al., 2022; Stewart, 1980). Briefly, lyophilized nanoparticles were dissolved in 2 mL of chloroform and then 2 mL of freshly prepared ammonium ferrothiocyanate was added. The resultant mixture was vigorously stirred for 15 min and then allowed to stand for at least 15–20 min to facilitate phase separation. The resultant lower chloroform layer containing the red complex of phospholipid and ferrothiocyanate was separated, and its absorbance was measured at $\lambda = 488$ nm by an RF-5301PC spectrofluorometer (Shimadzu, Italy). Each experiment was repeated at least three times. A calibration curve was obtained using mixtures of DPPC /DSPE-PEG_{2000} at concentrations ranging between 0.1 and 0.006 mg/mL.

2.5.4. Determination of drug loading (DL%)

The amount of Ilo loaded into each nanoparticle sample was evaluated by HPLC analysis using a method reported elsewhere (Craparo et al., 2024b). Briefly, a Waters Breeze System liquid chromatograph equipped with an autosampler (40 μL injection volume) and a Shimadzu UV − vis HPLC detector, was used, with a Luna C18 column (Phenomenex) and a mobile phase consisting of a mixture of acetonitrile (ACN) and aqueous solution at pH 3 (50:50), operating with a flow of 1 mL/min. The analysis was performed in isocratic conditions and the absorbance of Ilo was detected at 207 nm. The drug loading was calculated by comparing the sample's peak area with a calibration curve obtained from the HPLC analysis of Ilo standard solution at the concentration ranging from 0.04 to 0.01 mg/mL.

2.5.5. Release study

The drug release kinetic was determined by quantification of Ilo released from Ilo@PEG-LPHNPs over time, in simulated lung fluid (SLF3) (Marques et al., 2011), using the dialysis method. Briefly, a known amount of Ilo@PEG-LPHNPs was dispersed in 1 mL of PBS at pH 7.4 (10 mg/mL), placed in a dialysis tubing (MWCO 12 − 14 kDa), immersed in 10 mL of PBS at pH 7.4 containing 0.02 % wt of DPPC (SLF3) and then incubated at 37 °C under continuous stirring in an orbital shaker. At scheduled time intervals (0.5,1, 2, 4, 6, 12 and 24 h), dialysis tubing was removed by the external medium and placed in 10 mL of fresh medium. The external media collected were freeze-dried and Ilo extracted by dissolving the obtained powder in 1 mL of mobile phase used for HPLC, as described above. The dispersion was then filtered (PTFE filter, 0.45 μm), and analysed by HPLC to determine the released drug. Release curves were obtained by reporting the amount of % of the released drug as a function of incubation time. The release profile of Ilo alone (0.01 mg) was used as a control. Each experiment was carried out in triplicate and the results agreed within ± 5 % standard error.

2.5.6. Measurement of interactions with mucin

The interactions between each sample and mucin were determined by a turbidimetric assay (Craparo et al., 2024b). Briefly, a saturated solution of Type II mucin was prepared dispersing an excess of mucin in water (0.08 % w/v), under stirring overnight, followed by centrifugation at 6000 rpm, 4 °C for 20 min and collection supernatant. Then, each sample was dispersed in water at a concentration of 2 mg/mL and then, after complete dispersion, mixed 1:1 (v/v) with mucin dispersion obtaining a final nanoparticles concentration of 1 mg/mL. The light scattering of the mucin/sample mixtures was measured by spectrophotometric analysis at 650 nm at time 0 and after incubation for 30 and 60 min at 37 °C. The absorbance of mucin or sample dispersion in water was also evaluated as a control. Experiments were run in triplicate, and results are expressed as absorbance at 650 nm ± SD over time.

2.6. Microparticle production and characterization

2.6.1. Preparation of spray-dried microparticles (MPs) and Nano-into-Microparticles (NiM)

MPs and NiM formulations were prepared by using a Mini Spray Dryer B-290 (Buchi, Milan, Italy) and the following parameters: inlet T: 110 °C; outlet T: 60–66 °C; aspiration: 100 %; feed pump: 10 %; atomizer nozzle: 140 μm; used gas: compressed air. In detail, MPs made of mannitol alone were produced at two different mannitol concentrations (5 and 10 % w/v) in the liquid feed, in the presence of increasing amounts of AB as a porogen agent (0, 5, 10, 20, and 30 wt% relative to the weight of mannitol). While NiM formulation were produced using as feeding liquid a dispersion of PEG-LPHNPs and Ilo@PEG-LPHNPs (0.25 %w/v), in a 10 % w/v aqueous mannitol dispersion containing 10 % w/v of AB, obtaining respectively NiM and Nim@Ilo.

2.6.2. Particle morphology

The morphology of the particles was examined using SEM analysis (Phenom™ ProX Desktop SEM microscope, Thermo Fisher Scientific, Milan, Italy). Each sample was placed on double-sided adhesive tape, which was previously applied to a stainless-steel stub and then sputter-coated with gold (approximately 10 nm thick) prior to microscopy examination. The ImageJ program was utilized to calculate the particle

size distribution and geometric diameter (d_{geom}) for each sample from images by analysing more than 500 particles. The theoretical aerodynamic diameter (d_{aer}) was calculated using an equation reported elsewhere (Craparo et al., 2024a).

2.6.3. Tapped density (ρ_{tapp})

The ρ_{tapp} was measured by the syringe method, as already reported (Craparo et al., 2024a). Each powder was filled into a 1 mL graduated syringe and the powder amount determined by weight difference. Then, ρ_{tapp} was calculated from the volume value was determined by tapping the syringe onto a level surface from a height of 2.5 cm, 100 times until a constant volume was achieved. Each measurement was performed in triplicate.

2.6.4. Rheological analysis

Cystic fibrosis artificial mucus (CF-AM) was prepared as previously reported (Craparo et al., 2024b). Rheological properties of CF-AM alone or in the presence of Ilo@PEG-LHNPs, NiM@Ilo and MPs (2 mg/mL), were determined at 25 °C by using a rotational rheometer (TA Instruments) coupled to 8 mm parallel plate geometry and a controlled Peltier plate, maintaining a gap of 300 μm. Firstly, the linear viscoelastic region of CF-AM was determined by a strain sweep test ranging from 0.1 to 20 %, which was found to be in the range of 5–10 %. Then, a frequency sweep (0.1 − 2 Hz) was performed for all samples at 5 % constant strain to determine complex viscosity (η*). All rheological tests were conducted in triplicate, and Trios Software v3.3 TA Instruments was used for data acquisition and analysis.

2.6.5. Aerodynamic behaviour

The aerodynamic behaviour of NiM@Ilo was evaluated using an Handihaler® dry powder inhaler (DPI) connected to an Andersen Cascade 8 Stage Impactor (ACI, InPharmaTec) equipped with a pre-separator (PS) between stage −2 and the induction port.

To promote optimal particle deposition in each stage during powder aerosolization, the PS and impaction cups of each stage were coated with 1 % (w/v) of Tween 80® in ethanol before use and left to dry. The flow rate was set to 90 L/min.

Three manually filled methylcellulose capsules (size 3) each weighing 60 ± 0.1 mg, were sequentially introduced into the (ACI), with a discharge duration of 5 s each. Subsequently, the deposited powder in each stage was retrieved using 2 mL of water, and absorbance intensities were measured at a wavelength of 540 nm. NiM@Ilo's dispersions in water at different concentrations were used as standard.

For each sample, the experiment was repeated at least three times (3 capsules for each actuation), and the data obtained were analyzed to determine the emitted powder (EP; powder collected in the mouthpiece, in the IP, in the PS and the impaction cups) and the EP% (ratio between the EP and the initial mass of the tested sample). Furthermore, the fine particle fraction (FPF%), defined as the mass percentage of EP with an aerodynamic diameter less than 5.0 μm, was determined by interpolation of the cumulative aerodynamic diameter distribution curve. The cumulative mass of each stage was plotted as a percentage of the sample recovered relative to the cut-off diameter, excluding the mass deposited in the induction port due to the unavailability of a precise upper-size limit for particles deposited in this section. The mass median aerodynamic diameter (MMAD) and the value of the geometric standard deviation (GSD) of the particle's aerodynamic diameter were extrapolated from the graph according to the European Pharmacopeia (10th edition).

2.7. Biological characterization

2.7.1. Cell viability

The cytocompatibility of NiM, NiM@Ilo, and Mannitol matrix (MPs) was assessed by the tetrazolium salt (MTS) assay on macrophage (Raw 264.7), and human bronchial epithelium (16 HBE) cell lines, using a commercially available kit (Cell Titer 96 Aqueous One Solution Cell Proliferation assay, Promega). Cells were seeded in a 96-multiwell plate at density of $2{,}5 \times 10^4$ cells per well and grown in DMEM. After 24 h, the medium was replaced with 200 μL of fresh culture medium containing NiM, NiM@Ilo and MPs at different concentrations corresponding to equivalent concentrations of Iloprost of 25, 50, 100, 250 and 500 nM. After 24 and 48 h of incubation, samples were withdrawn from the wells and replaced with 100 μL of fresh medium and 20 μL of a MTS solution. Plates were incubated for an additional 2 h at 37 °C. Then, the absorbance at 490 nm was measured using a microplate reader (PlateReader AF2200, Eppendorf). To do this experiment, it was necessary to make isotonic the medium in which MPs, NiM and NiM@Ilo, were dispersed.

Free Iloprost dispersions at the same concentration were used as positive control, as untreated cells were used as negative control. In particular, to prepare the Ilo dispersion in DMEM, a stock solution of Ilo in DMSO (1 mg/mL) was prepared. The viability was expressed as the percentage obtained from the ratio between each sample with respect to their negative control (100 % of cell viability).

2.7.2. Cell uptake

The quantitative cellular uptake of PEG-LPHNPs samples was carried out on Raw 264.7 lines. Cells were seeded in a 96-multiwell plate at a density of 2.5×10^4 cells per well and grown in DMEM. After 24 h, cells were incubated with 0.036, 0.072, and 0.18 mg/mL (corresponding respectively to 25, 50 and 100 nM of Iloprost) for 1, 2, 6 and 24 h. Then, cells were lysed with 100 μL of lysis buffer (1 % Triton X-100, 2 % SDS in DPBS) and incubated for 2 h at room temperature. 75 μL of lysates were transferred to a disposable 96-well for fluorescence intensity measurements (λEX: 550 nm; λEX: 580 nm) on an Eppendorf plate reader spectrofluorophotometer. The remaining 25 μL of lysates were used for protein content determination with the bicinchoninic acid kit (Sigma Aldrich) according to the protocol of the manufacturer. Mean fluorescence intensity was calculated by correcting fluorescent signals for protein content, expressed as the ratio of fluorescence intensity (I.F.) per microgram of protein. The experiment was conducted in triplicate.

Additionally, to demonstrate the *stealth* properties of PEG-LPHNPs, the uptake of un-pegylated nanoparticles (LPHNPs) was also evaluated on Raw 264.7.

Finally, uptake was also evaluated by fluorescent microscopy (Zeiss "AXIO Vert. A1″ Microscope Inverted). In particular, Raw 264.7 cells were seeded at a density of 2.5×10^4 cells/well in an 8-well plate and cultured for 24 h. Subsequently, the medium was replaced with 500 μL of fresh DMEM containing 0.07 mg/mL of PEG-LPHNPs and LPHNPs, and cells were incubated for 6 and 24 h. After removal of the medium, the cell monolayer was washed twice with PBS pH 7.4, fixed with 4 % formaldehyde for 10 min, and washed again with DPBS. Cell nuclei were stained with 4′,6-diamidino-2-phenylindole (DAPI) for 10 min at room temperature. Images were captured using a fluorescence microscope with an Axio Cam MRm (Zeiss). Untreated cells were used as negative control to set the auto fluorescence.

2.7.3. Elisa test

To evaluate the anti-inflammatory effect of Iloprost entrapped into nasystems, an ELISA test was carried out, using interleukin-6 (IL-6) Human ELISA Kit from Cayman Chemical. 16-HBE cells were plated on a 96-well plate at a cell density of 2×10^4 cells/well in DMEM. After 24 h of incubation, the medium was removed and then the cells were co-treated for 24 h at 37 °C with DMEM containing10 μg/mL^{-} of LPS (Sigma-Aldrich) and free Iloprost, PEG-LPHNPs and Ilo@PEG-LPHNPs at different concentrations corresponding to Iloprost equivalent of 50 and 500 nM. After 24 h of incubation, the medium was removed, the cells were washed with DPBS and treated following the Il-6 ELISA kit protocol.

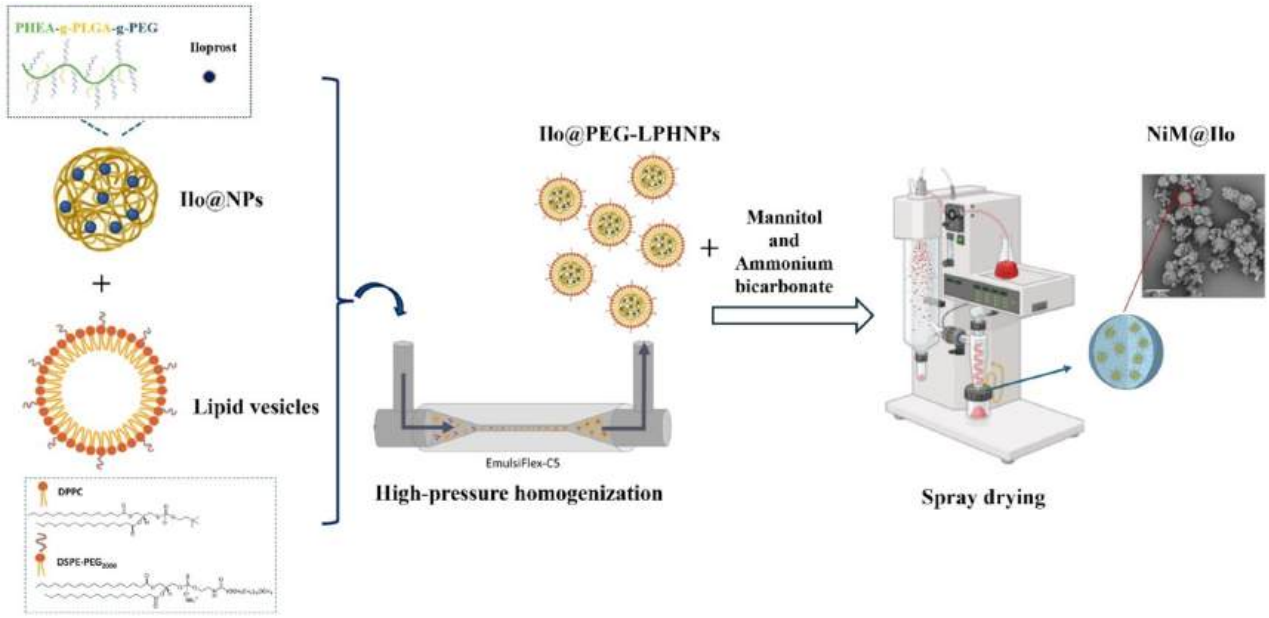

Scheme 1. Schematic representation of Ilo@LPHNPs production, and the NiM@Ilo production by the spray drying (SD) process.

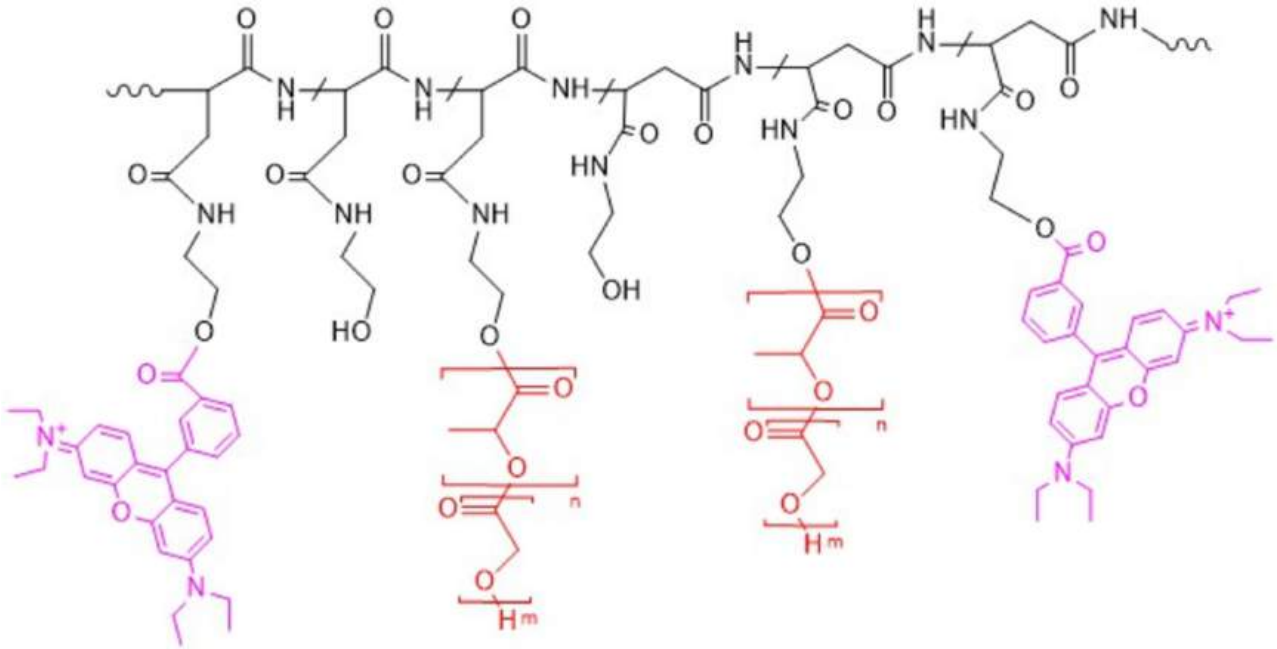

Fig. 1. Chemical structure of the PHEA-*g*-RhB-*g*-PLGA graft copolymer: PHEA backbone (black), RhB (fuchsia), PLGA (red, m = n = 92).

3. Result and Discussion

Based on our recent findings which demonstrate the anti-inflammatory effects of either free Iloprost (Ilo) or Ilo-loaded polymeric nanoparticles on the in vitro cell model of Cystic Fibrosis (CF), this work focuses on the realization and characterization of Nano-into Microparticles (NiM) entrapping Ilo-loaded lipid-polymer hybrid nanoparticles (Ilo@LPHNPs) (as schematically depicted in Scheme 1), with aerosolization properties suitable for inhalation thanks to the use of a proper amount of porogen, and the in vitro anti-inflammatory effect evaluation (Craparo et al., 2024a, 2024b). The use of NiM particles is justified by the need to optimize the pulmonary bioavailability of the drug and reduce its side effects in the approved clinical use for the treatment of pulmonary arterial hypertension (PAH), but also to open a new opportunity for its repositioning in the treatment of CF via inhalation (Boucetta et al., 2024).

3.1. Production of hybrid polymer-lipid nanoparticles containing Ilo (PEG-LPHNPs@Ilo)

To obtain the polymeric core of the hybrid polymer-lipid nanoparticles, a graft copolymer based on α,β-poly(N-2-hydroxyethyl)-DL-aspartamide/Rhodamine/poly-lactic-*co*-glycolic acid (PHEA-g-RhB-*g*-PLGA) was synthesized (Fig. 1) and characterised as previously described, resulting as degrees of derivatization in mole % of RhB (DD_{RhB}) and PLGA (DD_{PLGA}) relative to the moles of repeat units (U.R.)

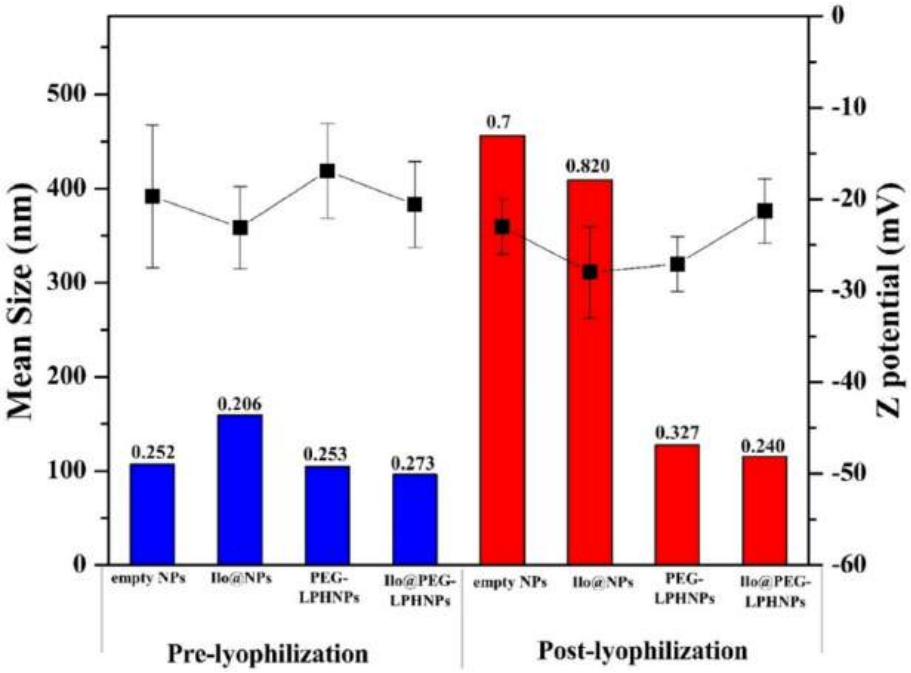

Fig. 2. Mean size, PDI (histogram) and ζ-potential (square symbol) of empty NPs, Ilo@NPs, PEG-LPHNPs and Ilo@PEG-LPHNPs, determined in twice distilled water, before and after freeze-drying (PDI indicates on each histogram).

in the copolymer PHEA equal to, respectively, 0.55 ± 0.05 % and 4.8 ± 0.2 % in moles, and in an average molecular weight ($\overline{M}_w$) equal to 130.5 kDa ($\overline{M}_w/\overline{M}_n = 1.2$) (Craparo et al., 2024b).

For the synthesis of the graft copolymer, PHEA was chosen as the hydrophilic polymeric backbone due to its remarkable water solubility and the reactivity of its primary hydroxyl groups, which can be easily functionalized. PLGA, a biocompatible and biodegradable polymer, was conjugated to the side chains of PHEA to introduce hydrophobicity to the final copolymer, enabling the formation of polymeric nanoparticles and the encapsulation of hydrophobic drugs. Finally, Rhodamine was chemically attached to obtain a fluorescent copolymer, allowing detection via fluorescence microscopy. Starting from the Ilo and/or the PHEA-*g*-RhB-*g*-PLGA organic dispersion, Ilo@NPs and empty NPs were obtained by the nanoprecipitation.

Specifically, the Iloprost free acid form was obtained from the commercial Endoprost® formulation, containing Iloprost tromethamine salt (0.05 mg/0.5 ml). To each vial, 20 μL of 0.01 M HCl was added, the obtained dispersion was stirred overnight to remove the ethanol present in the commercial preparation, and then freeze-dried. The resulting powder was used for further experiments. Characterization of both samples by using dynamic light scattering (DLS) showed a mean size, expressed as Z-Average, below 200 nm, with acceptable polydispersity. Data are shown in Fig. 2. From the figure, it can also be seen that the drying process through freeze-drying (a process necessary for the long-term preservation of the drug carriers), however, gave unsatisfactory results, as the freeze-dried product, once placed in an aqueous fluid, presents large aggregates, with high PDI values.

Compared to the previously described work where PEGylated polymeric nanoparticles were used to deliver Ilo, in this study, we aimed to prepare hybrid polymeric systems coated with a PEGylated lipid shell (Craparo et al., 2024b). The use of PEGylated phospholipids in the production of hybrid nanoparticles improves the surface properties of PEGylated nanoparticles, such as enhanced stability in biological fluids, reduced recognition and uptake by the immune system (particularly macrophages), and improved circulation time in the body. Additionally, PEGylation can increase the nanoparticles' ability to penetrate mucus barriers and enhance their overall biocompatibility and efficacy in delivering therapeutic agents. Consequently, this approach retains these key surface effects and results in systems that are more compatible with pulmonary tissues, easily dispersible, and provide even more controlled drug release in a simulated pulmonary fluid.

To obtain the surface pegylated LPHNPs, phospholipidic vesicles were produced by the Thin Layer Evaporation (TLE) starting from a mixture (3:1 wt:wt) of DPPC/DSPE-PEG_{2000}. Both DPPC and DSPE-PEG_{2000} were selected for their advantageous properties, well documented in the literature. Being the major phospholipid in human lung surfactant, DPPC plays a key role in pulmonary drug delivery systems and in studies of bilayers in the human body. It offers several favorable characteristics as a drug carrier, including high biocompatibility, avoidance of macrophage uptake, low production costs, and the ability to protect the active substance from degradation while modulating its release (Li et al., 2020). DSPE-PEG_{2000}, on the other hand, enhances the diffusion of hybrid nanoparticles through pulmonary mucus and provides stealth properties against macrophage cells by exposing PEG chains on the particle surface (Craparo et al., 2008; Guichard et al., 2017; Sanchez et al., 2017).

The empty and Ilo-loaded PEG-LPHNPs (named respectively PEG-LPHNPs and Ilo@PEG-LPHNPs) were prepared by using the high-pressure homogenization (HPH) method. This involved mixing aqueous dispersions of empty NPs or Ilo@NPs with phospholipidic vesicles, followed by isolation through ultracentrifugation.

After their preparation, both the hybrid samples, PEG-LPHNPs and Ilo@PEG-LPHNPs, were characterized by determining the average size, PDI, and zeta potential in aqueous dispersion. The obtained values, also reported in Fig. 2, show that the samples have an average size of approximately 100 nm. Although these values are comparable to those of NPs, after freeze-drying, the hybrid systems give rise to homogeneous dispersions, with particle size comparable to that immediately after preparation; on the contrary, the polymeric NPs, in the absence of phospholipidic shell, are difficult to disperse. Therefore, the lipid shell surrounding the polymer nanoparticles reduces interactions between the polymer chains. This minimizes aggregation during the lyophilization process, ensuring that both PEG-LPHNPs and Ilo@PEG-LPHNPs remain non-aggregated and thereby enhancing their re-dispersibility in aqueous medium. Fig. 2 also includes the pre- and post-lyophilization ζ-potential

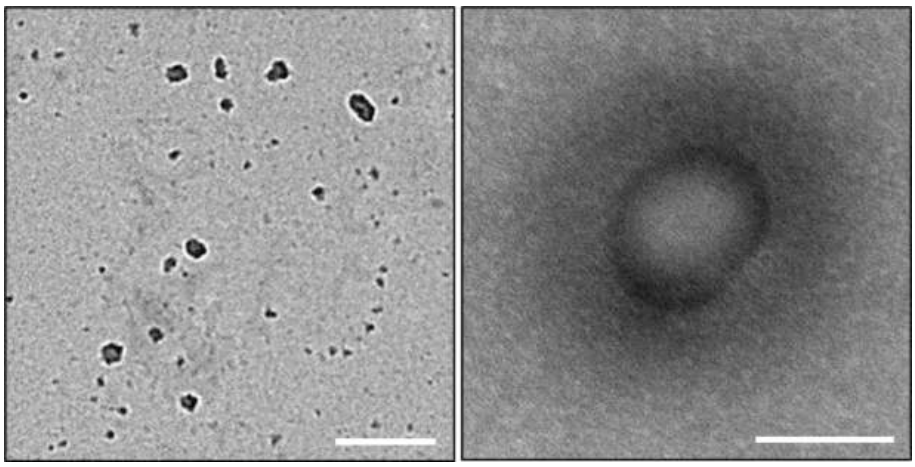

Fig. 3. TEM images of Ilo@PEG-LPHNPs sample; the bar represents: 500 nm (left), 200 nm (right).

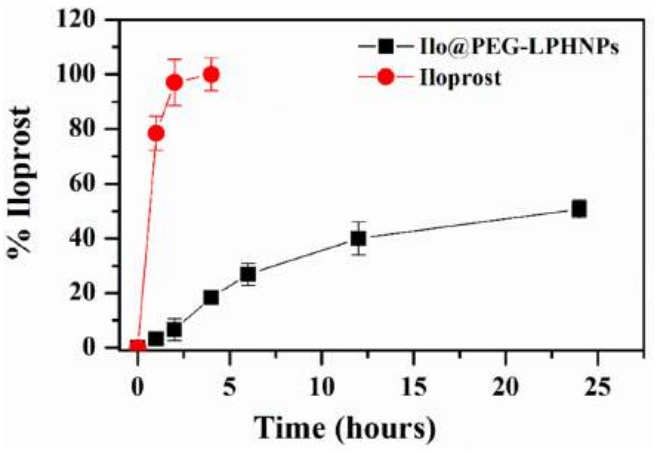

Fig. 4. Drug release profile (black) from sample Ilo@PEG-LPHNPs in simulated lung fluid (SLF4, 0.02 % w/v DPPC), under sink conditions and Iloprost dissolution profile (red) (n = 3).

values in Milli-Q water, which are negative for all samples both before and after the drying process, minimally influenced by the process in the case of loaded systems.

In the literature, the few reported examples of pulmonary delivery systems for Ilo are liposomes, which exhibited large sizes and were dependent on the aerosolization system (Jain et al., 2014; Kleemann et al., 2007).

To evaluate the morphology, TEM analysis was conducted (Fig. 3), which revealed a core–shell structure, as hypothesized considering the stepwise production procedure of the hybrid systems.

As reported for similar hybrid polymer-lipid systems, the formation of core–shell nanoparticles occurred by interactions between the lipids and the copolymer, which affect the sol–gel transition temperature of phospholipids, as highlighted by DSC analysis. (Craparo et al., 2024a, 2022).

The phospholipids amount effectively incorporated into the core/shell structure of the hybrid nanoparticles, quantified by the ammonium iron thiocyanate colorimetric assay (Stewart, 1980), was equal to 64 wt % for the Ilo@PEG-LPHNPs sample; while the drug content, quantified by the HPLC method described in the experimental part and expressed as Drug Loading (DL%, the ratio between the weight quantity of incorporated Iloprost and the total sample weight), resulted equal to 0.125 wt%, corresponding to EE% of 75 wt%.

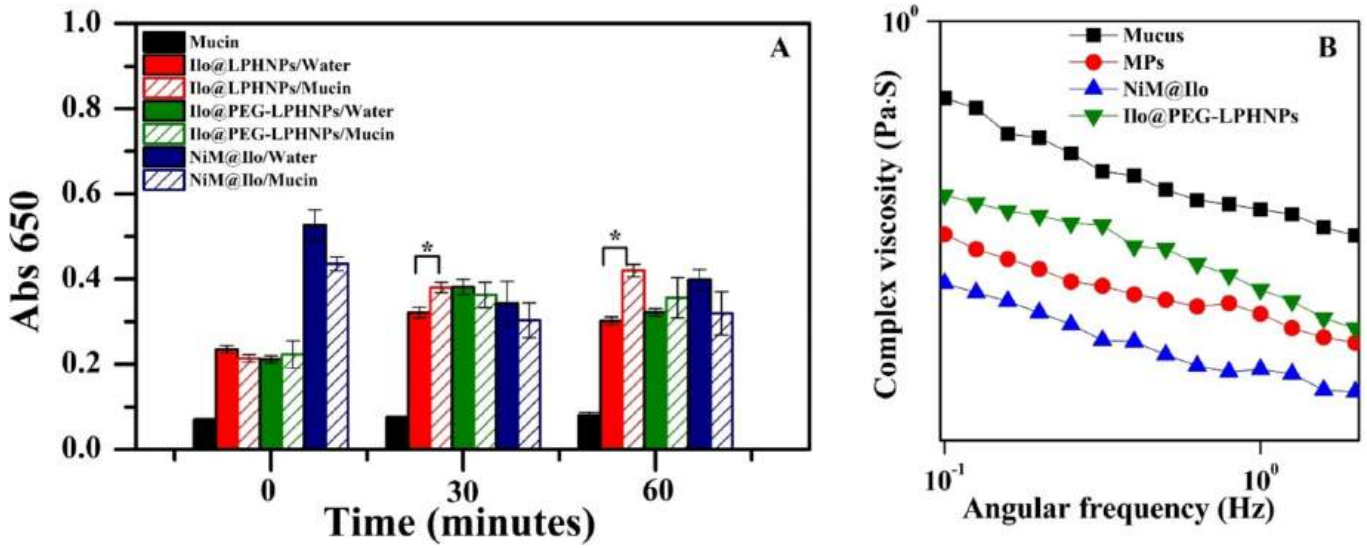

Fig. 5. (A) Transmittance at 650 nm of dispersions containing mucin alone, Ilo@PEG-LPHNPs, Ilo@LPHNPs and NiM@Ilo samples, in water or in mucin dispersion; **(B)** complex viscosity (η*) of CF-AM alone (black) and treated with NiM@Ilo (blue), MPs (red, matrix) and Ilo@PEG-LPHNPs (green), (x ± 5 %) (n = 3).

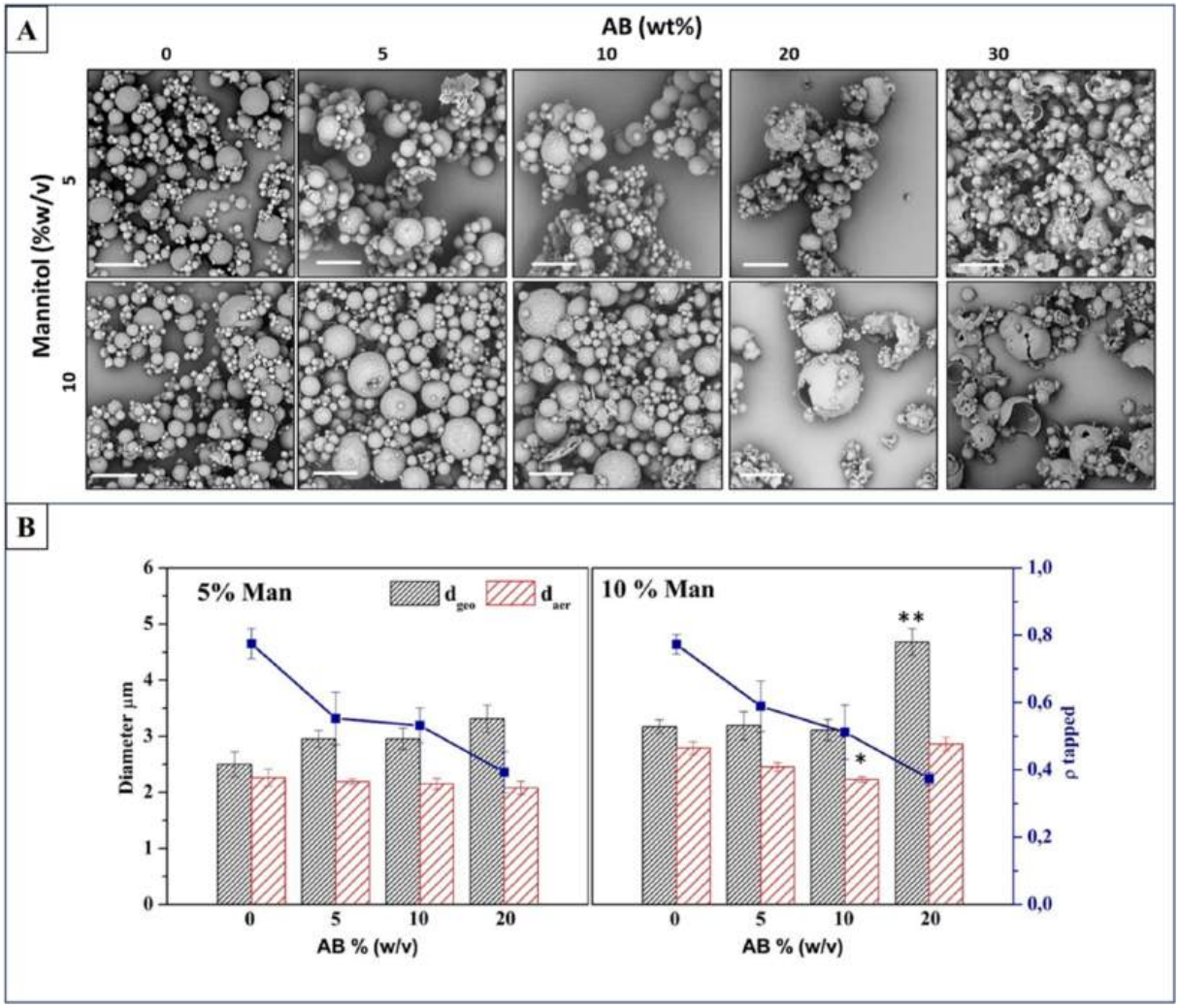

Fig. 6. (**panel A**) SEM images of microparticle samples (MPs) obtained at 5 and 10 wt% of mannitol concentrations and AB concentrations ranging between 0, 5, 10, 20, and 30 % w/v, at a magnification of 4000x (the bar represents 10 µm); (**panel B**) Geometric diameter (d_{geo}), theoretical aerodynamic diameter (d_{aer}) and tapped density (ρ_{tapped}) of MPs obtained with 5 wt% (left) and 10 wt% (right) of mannitol, as a function of the AB percentage (0, 5, 10 and 20 % w/v). (*$p < 0.05$, d_{aer} value of sample obtained with AB 10 % w/v vs those obtained with AB 0, 5, 20 % w/v; **$p < 0.01$, d_{geom} value of sample obtained with AB 20 % w/v vs those obtained with AB 0, 5, 10 % w/v;).

To demonstrate that the drug incorporated into the hybrid nanostructure is able to diffuse once the resulting system is dispersed in an aqueous fluid, a cumulative release study was conducted in simulated lung fluid (SLF4, 0.02 % w/v DPPC), under sink conditions, and reported in Fig. 4 as percentage of the released drug as a function of the incubation time (Marques et al., 2011).

It showed that Ilo is released from Ilo@PEG-LPHNPs in a prolonged manner in the SLF medium, without exhibiting a burst effect, reaching 50 wt% of the incorporated amount in approximately 24 h incubation. This behaviour, i.e the drug release over an extended period, could represent a significant advantage in the potential use of hybrid nanoparticles for the pulmonary administration of Ilo, because this feature may reduce the need for frequent administrations while potentially minimizing side effects resulting from systemic drug biodistribution.

Compared to the previously described PEGylated polymeric particles, the hybrid systems exhibit an even slower release (Craparo et al., 2024b). Specifically, the amount released from the polymeric and hybrid systems is approximately 40 and 28 wt% of the incorporated amount, respectively, after 6 h of incubation. Such slower release kinetics can be explained by considering the presence of an additional diffusion layer, with different chemical-physical characteristics compared to the polymeric particles. Therefore, the introduction of an external lipid shell in the nanoparticulate system indeed modifies the drug release capacity from the polymeric particle core.

Regarding the liposomal systems described in the literature for the delivery of Ilo, they show both a significantly lower DL and EE compared to the systems we described (Jain et al., 2014; Kleemann et al., 2007). Therefore, the hydrophobic nature of the drug allows for greater incorporation within the nanoparticle core of the hybrid systems described in this work compared to liposomal systems present in the literature.

Being designed for pulmonary administration, it was useful to investigate the ability of Ilo@PEG-LPHNPs to avoid interaction with mucus once they reached the affected lung region. This characteristic allows the hybrid nanoparticles to diffuse through the mucus and reach the epithelial layer, the drug target. Therefore, a study was conducted using UV turbidimetry spectroscopy (Fig. 5A), where any increase in absorbance at 650 nm is indicative of interaction between particles and mucin (Abruzzo et al., 2021). As shown, there are no significant differences in the Abs values registered in the presence and absence of mucin, which confirms, as with the recently described PEGylated polymeric nanoparticles, that PEG has a reducing effect on interactions with mucus components. These data were further supported by experiments conducted with non-PEGylated LPHNPs, which showed a significant

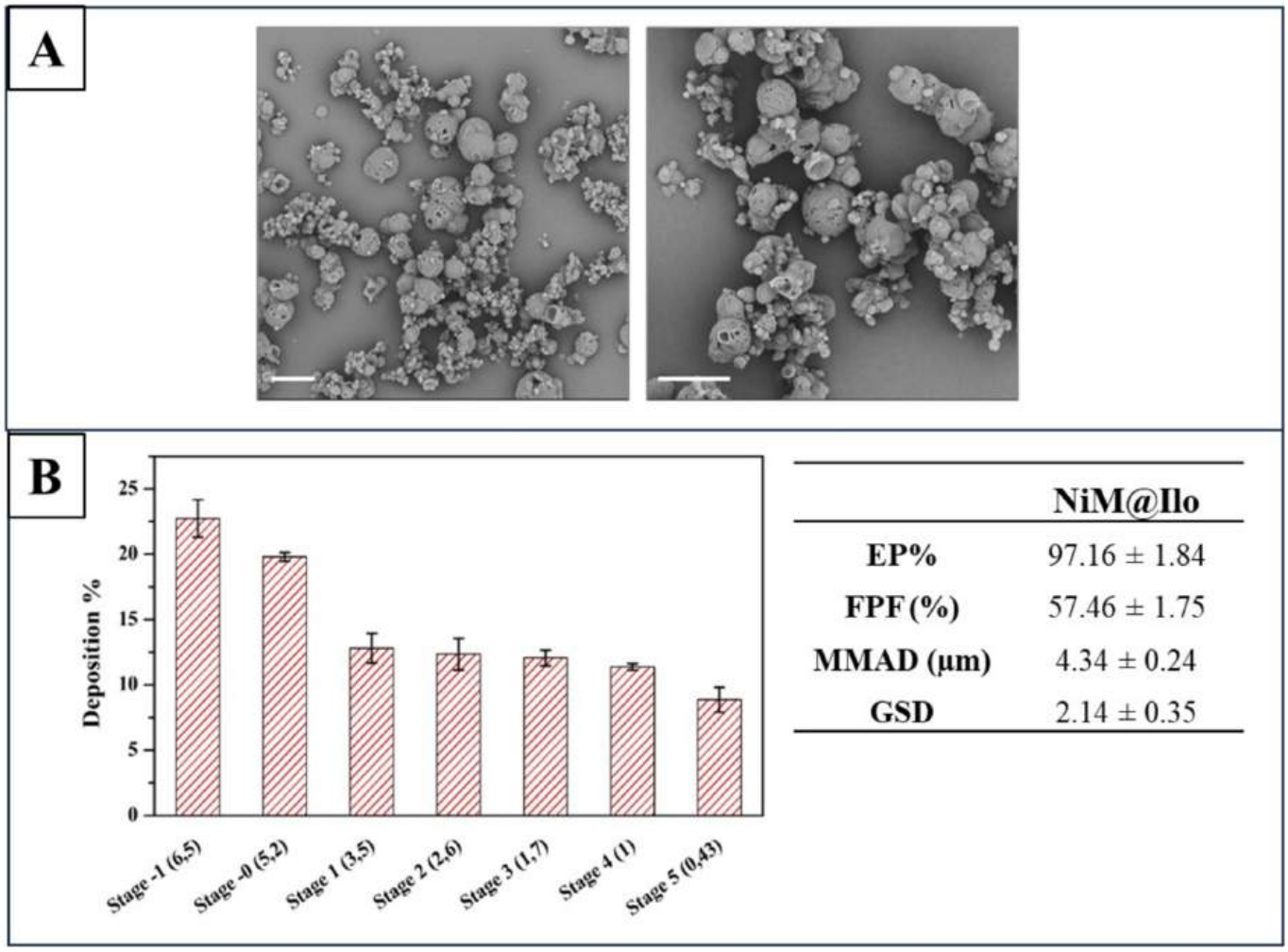

Fig. 7. (**panel A**) SEM image of the NiM@Ilo sample at magnification: 3000x (left) and 5000x (right) (the bar represents 10 μm); (**panel B**) Deposition of NiM@Ilo samples on the stages of the ACI after testing with Breezhaler ® at a flow rate of 90 L/min (* $p < 0.05$). Aerodynamic parameters of the tested samples: emitted powder (EP%), fine particle fraction (FPF), mass median aerodynamic diameter (MMAD), geometric standard deviation (GSD). Values represent mean ± SD (n = 3).

increase in absorbance when LPHNPs were incubated with mucin compared to water. This increase is due to the interaction between the LPHNPs and mucin, highlighting the efficacy of PEGylation in reducing nanoparticle-mucin interactions.

Furthermore, a rheological measurement between cystic fibrosis artificial mucus (CF-AM) alone and that where the Ilo@PEG-LPHNPs were dispersed shows a significant reduction in the complex viscosity of the latter, further confirming the positive effect on the viscous properties of the mucus itself (Fig. 5**B**).

Hence, these hybrid systems exhibit outstanding capabilities for efficiently loading and releasing the Ilo, associated with a marked ability to reduce mucus viscosity. Moreover, they can undergo freeze-drying and subsequent redispersion in an aqueous medium, resulting in a particle dispersion of around 100 nm. Consequently, these systems hold promise for the preparation of a liquid suitable for extemporaneous nebulization into the lung tree. In this case, the deposition will be governed solely by the device used for nebulization, which requires complex transport mechanisms and long administration times.

3.2. Production of inhalable nano into microparticles (NiM)

Therefore, we developed a dry powder formulation that could improve deposition efficiency and reduce administration times, optimizing the system for more practical and effective use. Given the colloidal size, it was necessary to incorporate the hybrid systems into micrometric matrices with characteristics suitable for aerosolization, to be inhaled using dry powder inhaler devices.

Mannitol was chosen for its stability under processing conditions, pharmaceutical safety, and suitability for pulmonary use due to its notable rehydrating properties in the airways (Chen et al., 2016).

Therefore, through the optimization of a spray drying (SD) process, microparticles were produced. Compared to the previous work where we used only mannitol, in this case, we used a porogen agent such as ammonium bicarbonate (AB) to modulate the aerodynamic properties and flow characteristics. The latter was chosen to modulate particle characteristics such as density and porosity, because it degrades at the operating SD temperature (110 °C), producing CO_2, H_2O, and NH_3, and is therefore removed simultaneously with the formation of microparticles, where it creates pores and bubbles (Ghosh Dastidar et al., 2018). In detail, different MPs samples were produced by SD using aqueous solutions of mannitol at two concentrations (5 and 10 wt%) as liquid feed, containing AB in increasing quantities ranging from 0 wt% to 30 wt% related to the mannitol weight. SEM images of obtained matrices (MPs) are reported in Fig. 6**, panel A**.

As observed in the absence of the porogen, the MPs exhibit a spherical shape without surface pores. As the AB amount increases from 5 to 30 wt%, both the sample polydispersity and morphology changed, featuring the surface progressively larger pores and losing the particle sphericity, so that particles appear fused together with AB 30 wt%. For this reason, the latter sample was not further characterized.

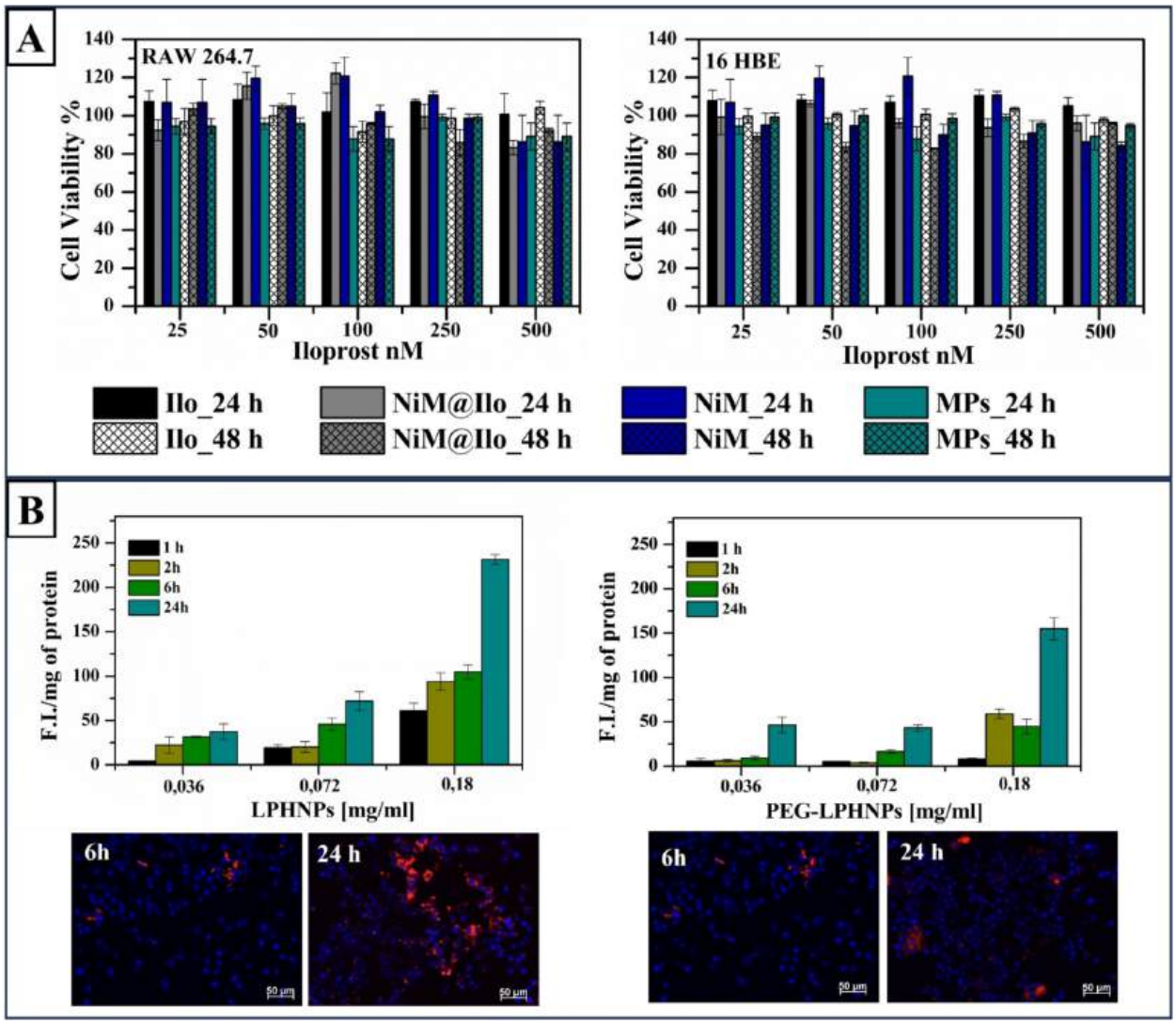

Fig. 8. (panel A) Cytotoxicity of NiM@Ilo, NiM and MPs on 16-HBE and RAW 264.7 cell lines, as a function of Ilo concentrations (in nM), after 24 (left) and 48 h (right) incubation. Data represent the mean ± SD of 2 experiments conducted each with four replicates; **(panel B)** Hybrid nanoparticles uptake by RAW 264.7 cells as a function of incubation time and LPHNPs or PEG-LPHNPs concentration, expressed as intracellular fluorescence.

To gather information on the aerodynamic behaviour of the obtained MPs, the theoretical aerodynamic diameter (d_{aer}) was determined. This value is obtained using a formula (outlined in the experimental section) based on the geometric diameter (d_{geo}) and the tapped density (ρ_{tapp}). Specifically, for all samples (5–20 wt% AB), d_{geo} values were calculated from SEM images using ImageJ software, and ρ_{tapp} was determined using the syringe method, as described in the experimental section (Tang and Perepezko, 2018). The results obtained are presented in Fig. 6, **panel B**.

From the analysis of the obtained values, it is evident that, starting from a mannitol concentration in the feeding solution of 5 % w/v, the d_{geo} of the particles not significantly increases with the increasing amount of AB used. However, when using a doubled mannitol concentration (10 % w/v), the particle d_{geo} significantly increases in the presence of 20 wt% of porogen in the feeding solution. The ρ_{tapp} values, on the other hand, significantly decrease with the increasing amount of AB at both mannitol concentrations in the feeding solution (5 % and 10 % w/v).

Based on these data and applying the formula (1) described in the experimental section, it was possible to calculate the theoretical d_{aer} values for each sample, also reported in Fig. 6 (**panel B**).

Analysing all the values to select a matrix to incorporate the hybrid nanoparticles, the choice fell on the matrix obtained from 10 % w/v mannitol with 10 wt% AB because it shows the significantly lowest theoretical d_{aer} value and the highest powder yield, equal to 55.7 wt%. Moreover, it shows the higher flowability (61.7 % vs 58.5 %) expressed as the Carr index (calculated using the following formula) (Pandey et al., 2023):

$$Carr\ Index = (\rho_{tapp} - \rho_{bulk})/\rho_{tapp} \times 100$$

Therefore, NiM@Ilo were produced through SD, using as feeding liquid a dispersion of Ilo@PEG-LPHNPs (0.25 % w/v), in a 10 % w/v aqueous mannitol dispersion, and adding 10 % w/v of AB. Furthermore, in the same way, starting to a dispersion of PEG-LPHNPs as feeding liquid, microparticles without the drug, named NiM, were prepared as control.

SEM analysis of the obtained NiM@Ilo (Fig. 7**, panel A**) highlights particles with a spherical shape, a rough surface, and rich in pores, thus exhibiting different characteristics compared to the MPs (microparticles made only of mannitol) showed in Fig. 6, panel A.

To gather information on the aerodynamic properties the NiM@Ilo particles, they were also characterized by determining d_{geo}, ρ_{tapp} and theoretical d_{aer} values, which resulted respectively equal to 3.27 μm, 0.465 g/mL, and 2.23 μm. Therefore, the presence of Ilo@LPHNPs influences the particle morphology (being porous, rough, and not perfectly

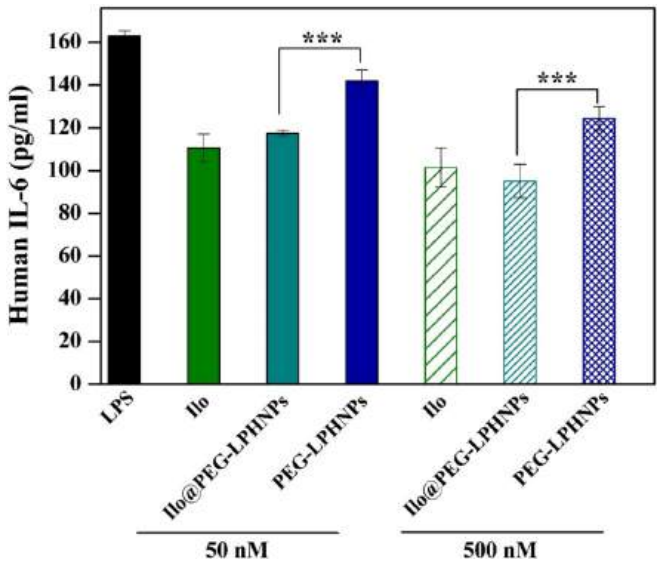

Fig. 9. Evaluation of Ilo, free or loaded into PEG-LPHNPs, and empty PEG-LPHNPs effects on 16-HBE cells as cytokine IL-6 production by Elisa test. ***$p < 0.001$.

spherical) but it has minimal effects on the other parameters of the empty microparticles such as d_{geom} and theoretical d_{aer} values, being the technological properties related to the aerosolization capability substantially unchanged.

An evaluation of the aerodynamic properties was also carried out on the NiM@Ilo sample using an Andersen cascade impactor (ACI). The results in terms of deposition pattern and aerodynamic parameters are shown in Fig. 7, **panel B**.

As can be seen, the results in terms of fine particle fraction (FPF%) and MMAD are very promising, being respectively equal to 57.46 % and 4.34 μm, the latter falling within the optimal dimensional range for efficient deposition in the bronchial tree. Therefore, the NiM@Ilo particles exhibit suitable aerodynamic properties for aerosolization into the lungs.

To demonstrate that the mannitol matrix at the deposition site can dissolve and release the Ilo@PEG-LPHNPs, a dissolution test was performed. This test aimed to evaluate if PEG-LPHNPs@Ilo dispersion could be successfully recovered from NiM@Ilo after dispersion in an aqueous fluid. The resulting dispersion was characterized by measuring the average size, polydispersity index (PDI), and ζ potential. The results were compared with those obtained from lyophilised LPHNPs@Ilo dispersion in water. Since the results are almost superimposable, except for a slight increase in PDI, it can be stated that the SD process does not alter the physicochemical characteristics of LPHNPs (data not shown).

Regarding the interactions with mucin/mucus at the deposition site, the presence of the mannitol matrix does not affect the interaction of Ilo@PEG-LPHNPs with mucin chains in the turbidimetric test (Fig. 5**A**), while it significantly reduces the complex viscosity of CF-AM compared to the nanoparticles alone (Fig. 5**B**).

3.3. Biological characterization

Once the aerosolizability of NiM@Ilo particles was established, the effects of their presence on the cell viability of 16-HBE and RAW 264.7 macrophage cells were determined after 24 and 48 h of incubation. In particular, the cytocompatibility of NiM@Ilo, NiM particles (microparticles containing empty hybrid systems) and MPs were evaluated by incubating the cells at different concentrations corresponding to equivalent concentrations of Ilo of 25, 50, 100, 250 and 500 nM. The results, shown in Fig. 8**, panel A**, indicate the absence of toxicity at all tested concentration levels and incubation times.

Furthermore, we evaluated the ability of PEG-LPHNPs to escape uptake by RAW macrophage cells, using hybrid particles made with only DPPC (non-PEGylated) as a control, named LPHNPs, as a function of incubation time and concentration. The results, shown in Fig. 8**, panel B**, as internalized fluorescence (due to RhB covalently linked to the copolymer), indicate that the internalization of both PEGylated and non-PEGylated particles is time- and concentration-dependent. Additionally, the internalization process is significantly lower for the PEGylated hybrid nanoparticles (PEG-LPHNPs), as seen in the microscope images where the particles are visualized by red spots after 6 and 24 hrs incubation. These results underscore the effectiveness of PEG in reducing macrophage internalization, giving the systems stealth properties.

Moreover, by using an ELISA test specific for human interleukin 6 (IL-6), we demonstrated that the efficacy of Ilo carried by the hybrid nanoparticles (sample PEG-LPHNPs@Ilo) in reducing its production in 16-HBE cells was comparable to that achieved by the free drug and significantly higher than that observed with empty hybrid particles (sample PEG-LPHNPs).

The results, expressed as the amount of IL-6 released, are shown in Fig. 9, based on two drug concentrations (50 and 500 nM).

4. Conclusion

In this study, we aimed to optimize a microparticle-based formulation for delivering Iloprost (Ilo) to the lungs, targeting inflammation in diseases like Cystic Fibrosis (CF). Previous research showed that Iloprost loaded into PEGylated polymeric nanoparticles could downregulate inflammatory cytokines similarly to the free drug (Craparo et al., 2024b).

Our latest study takes this a step further by using hybrid polymer-lipid nanoparticles as the drug carrier. These nanoparticles can be dried and easily re-dispersed in physiological fluids, providing a slow drug release that could reduce dosing frequency and side effects compared to commercial formulations. Notably, the PEGylated lipid in these hybrid nanoparticles seems to prevent interaction with mucin, as well as to reduce the complex viscosity of Cystic Fibrosis artificial mucus (CF-AM).

To create an aerosolizable powder suitable for lung delivery, we produced mannitol microparticulate matrices via spray drying, carefully selecting the liquid feed composition, including mannitol and ammonium bicarbonate (AB). This resulted in particles with ideal aerodynamic properties for lung deposition. The Nano-into-Microparticles were then produced by embedding the Ilo@PEG-LPHNPs. Tests confirmed that the NiM@Ilo particles had the right aerodynamic diameter and flowability for pulmonary administration, along with a significant reduction in CF-AM viscosity compared to the hybrid nanoparticles alone.

Biological testing showed that these surface PEGylated hybrid nanoparticles are biocompatible and less likely to be phagocytosed by macrophages compared to non-PEGylated particles. Importantly, the drug in these nanoparticles effectively exerted its anti-inflammatory effects, with interleukin 6 used as a model cytokine.

CRediT authorship contribution statement

Cinzia Scialabba: Writing – original draft, Investigation, Formal analysis. **Emanuela F. Craparo:** . **Marta Cabibbo:** Investigation, Formal analysis. **Salvatore Emanuele Drago:** Investigation, Formal analysis. **Gennara Cavallaro:** Supervision, Conceptualization.

Declaration of competing interest

The authors declare that they have no known competing financial interests or personal relationships that could have appeared to influence the work reported in this paper.

Data availability

Data will be made available on request.

Acknowledgment

Authors thank ATeNCenter of University of Palermo - Laboratory of Preparation and Analysis of Biomaterials for analysis instruments, and Mr. Francesco Paolo Bonomo for technical support.

Authors thank Dr Paola Riccobelli of the Department of Molecular and Translational Medicine, University of Brescia, Dr Lorena Giugno and Dr Stefania Castrezzati of the Division of Anatomy and Physiopathology, Department of Clinical and Experimental Sciences, University of Brescia, for transmission electron microscopy (TEM) analysis.

The research leading to these results has received funding from the European Union - NextGenerationEU through the Italian Ministry of University and Research under PNRR - M4C2-I1.3 Project PE_00000019: " Health Extended ALliance for Innovative Therapies, Advanced Lab-research, and Integrated Approaches of Precision Medicine - HEAL ITALIA" to Gennara Cavallaro. CUP: B73C22001250006 The views and opinions expressed are those of the authors only and do not necessarily reflect those of the European Union or the European Commission. Neither the European Union nor the European Commission can be held responsible for them.

References

Abruzzo, A., Giordani, B., Miti, A., Vitali, B., Zuccheri, G., Cerchiara, T., Luppi, B., Bigucci, F., 2021. Mucoadhesive and mucopenetrating chitosan nanoparticles for glycopeptide antibiotic administration. Int. J. Pharm. 606, 120874. https://doi.org/10.1016/j.ijpharm.2021.120874.

Boucetta, H., Zhang, L., Sosnik, A., He, W., 2024. Pulmonary arterial hypertension nanotherapeutics: New pharmacological targets and drug delivery strategies. J. Control. Release. https://doi.org/10.1016/j.jconrel.2023.11.012.

Chen, L., Okuda, T., Lu, X.Y., Chan, H.K., 2016. Amorphous powders for inhalation drug delivery. Adv. Drug Deliv. Rev. https://doi.org/10.1016/j.addr.2016.01.002.

Chvatal, A., Ambrus, R., Party, P., Katona, G., Jójárt-Laczkovich, O., Szabó-Révész, P., Fattal, E., Tsapis, N., 2019. Formulation and comparison of spray dried non-porous and large porous particles containing meloxicam for pulmonary drug delivery. Int. J. Pharm. 559, 68–75. https://doi.org/10.1016/j.ijpharm.2019.01.034.

Cipolla, D., Chan, H.K., 2018. Current and emerging inhaled therapies of repositioned drugs. Adv. Drug Deliv. Rev. https://doi.org/10.1016/j.addr.2018.09.008.

Craparo, E.F., Pitarresi, G., Bondi, M.L., Casaletto, M.P., Licciardi, M., Giammona, G., 2008. A nanoparticulate drug-delivery system for rivastigmine: Physico-chemical and in vitro biological characterization. Macromol. Biosci. 8, 247–259. https://doi.org/10.1002/mabi.200700165.

Craparo, E.F., Cabibbo, M., Scialabba, C., Giammona, G., Cavallaro, G., 2022. Inhalable formulation based on lipid-polymer hybrid nanoparticles for the macrophage targeted delivery of roflumilast. Biomacromolecules 23, 3439–3451. https://doi.org/10.1021/acs.biomac.2c00576.

Craparo, E.F., Cabibbo, M., Scialabba, C., Casula, L., Lai, F., Cavallaro, G., 2024a. Rapamycin-based inhaled therapy for potential treatment of COPD-related inflammation: production and characterization of aerosolizable nano into micro (NiM) particles. Biomater. Sci. 12, 387–401. https://doi.org/10.1039/d3bm01210g.

Craparo, E.F., Cabibbo, M., Scialabba, C., Laselva, O., Daniello, V., Di Gioia, S., Conese, M., Cavallaro, G., 2024b. Lung disease management by iloprost-loaded nanoparticles to address hyperinflammation associated with cystic fibrosis. ACS Appl. Nano Mater. 7, 14077–14089. https://doi.org/10.1021/acsanm.4c01379.

Etter, E.L., Mei, K.C., Nguyen, J., 2021. Delivering more for less: nanosized, minimal-carrier and pharmacoactive drug delivery systems. Adv. Drug Deliv. Rev. 179, 113994. https://doi.org/10.1016/j.addr.2021.113994.

Ewert, R., Gläser, S., Bollmann, T., Schäper, C., 2011. Inhaled iloprost for therapy in pulmonary arterial hypertension. Exp. Rev. Respir. Med. https://doi.org/10.1586/ers.11.14.

Gaikwad, S.S., Pathare, S.R., More, M.A., Waykhinde, N.A., Laddha, U.D., Salunkhe, K.S., Kshirsagar, S.J., Patil, S.S., Ramteke, K.H., 2023. Dry Powder Inhaler with the technical and practical obstacles, and forthcoming platform strategies. J. Control. Release. https://doi.org/10.1016/j.jconrel.2023.01.083.

Gessler, T., 2018. Inhalation of repurposed drugs to treat pulmonary hypertension. Adv. Drug Deliv. Rev. 133, 34–44. https://doi.org/10.1016/j.addr.2018.06.003.

Gessler, T., 2019. Iloprost delivered via the BREELIBTM nebulizer: a review of the clinical evidence for efficacy and safety. Ther. Adv. Respir. Dis. https://doi.org/10.1177/1753466619835497.

Ghosh Dastidar, D., Saha, S., Chowdhury, M., 2018. Porous microspheres: synthesis, characterisation and applications in pharmaceutical & medical fields. Int. J. Pharm. 548, 34–48. https://doi.org/10.1016/j.ijpharm.2018.06.015.

Giammona, G., Pitarresi, G., Craparo, E.F., Cavallaro, G., Buscemi, S., 2001. New biodegradable hydrogels based on a photo-cross-linkable polyaspartamide and poly (ethylene glycol) derivatives. Release studies of an anticancer drug. Colloid Polym. Sci. 279, 771–783. https://doi.org/10.1007/s003960100492.

Gonsalves, A., Menon, J.U., 2024. Impact of nebulization on the physicochemical properties of polymer-lipid hybrid nanoparticles for pulmonary drug delivery. Int. J. Mol. Sci. 25. https://doi.org/10.3390/ijms25095028.

Guichard, M.J., Leal, T., Vanbever, R., 2017. PEGylation, an approach for improving the pulmonary delivery of biopharmaceuticals. Curr. Opin. Colloid Interface Sci. https://doi.org/10.1016/j.cocis.2017.08.001.

He, Y., Liang, Y., Han, R., Lu, W.L., Mak, J.C.W., Zheng, Y., 2019. Rational particle design to overcome pulmonary barriers for obstructive lung diseases therapy. J. Control. Release. https://doi.org/10.1016/j.jconrel.2019.10.035.

Jain, P.P., Leber, R., Nagaraj, C., Leitinger, G., Lehofer, B., Olschewski, H., Olschewski, A., Prassl, R., Marsh, L.M., 2014. Liposomal nanoparticles encapsulating iloprost exhibit enhanced vasodilation in pulmonary arteries. Int. J. Nanomed. 9, 3249–3261. https://doi.org/10.2147/IJN.S63190.

Keshavarz, A., Kadry, H., Alobaida, A., Ahsan, F., 2020. Newer approaches and novel drugs for inhalational therapy for pulmonary arterial hypertension. Exp. Opin. Drug Deliv. https://doi.org/10.1080/17425247.2020.1729119.

Khalili, L., Dehghan, G., Sheibani, N., Khataee, A., 2022. Smart active-targeting of lipid-polymer hybrid nanoparticles for therapeutic applications: Recent advances and challenges. Int. J. Biol. Macromol. https://doi.org/10.1016/j.ijbiomac.2022.05.156.

Kleemann, E., Schmehl, T., Gessler, T., Bakowsky, U., Kissel, T., Seeger, W., 2007. Iloprost-containing liposomes for aerosol application in pulmonary arterial hypertension: formulation aspects and stability. Pharm. Res. 24, 277–287. https://doi.org/10.1007/PL00022055.

Li, Z., Qiao, W., Wang, C., Wang, H., Ma, M., Han, X., Tang, J., 2020. DPPC-coated lipid nanoparticles as an inhalable carrier for accumulation of resveratrol in the pulmonary vasculature, a new strategy for pulmonary arterial hypertension treatment. Drug Deliv. 27, 736–744. https://doi.org/10.1080/10717544.2020.1760962.

Marques, M.R.C., Loebenberg, R., Almukainzi, M., 2011a. Simulated biological fluids with possible application in dissolution testing. Dissolut. Technol. 18, 15–28. https://doi.org/10.14227/DT180311P15.

Neary, M.T., Mulder, L.M., Kowalski, P.S., MacLoughlin, R., Crean, A.M., Ryan, K.B., 2024. Nebulised delivery of RNA formulations to the lungs: From aerosol to cytosol. J. Control. Release. https://doi.org/10.1016/j.jconrel.2023.12.012.

Pandey, S., Premjit, Y., Khuntia, A., Kadival, A., Mitra, J., 2023. Development of probiotic-loaded calcium alginate-maltodextrin microparticles based on electrohydrodynamic technique. Powder Technol 428. https://doi.org/10.1016/j.powtec.2023.118808.

Pelaz, B., Alexiou, C., Alvarez-Puebla, R.A., Alves, F., Andrews, A.M., Ashraf, S., Balogh, L.P., Ballerini, L., Bestetti, A., Brendel, C., Bosi, S., Carril, M., Chan, W.C.W., Chen, C., Chen, X., Chen, X., Cheng, Z., Cui, D., Du, J., Dullin, C., Escudero, A., Feliu, N., Gao, M., George, M., Gogotsi, Y., Grünweller, A., Gu, Z., Halas, N.J., Hampp, N., Hartmann, R.K., Hersam, M.C., Hunziker, P., Jian, J., Jiang, X., Jungebluth, P., Kadhiresan, P., Kataoka, K., Khademhosseini, A., Kopeček, J., Kotov, N.A., Krug, H.F., Lee, D.S., Lehr, C.M., Leong, K.W., Liang, X.J., Lim, M.L., Liz-Marzán, L.M., Ma, X., Macchiarini, P., Meng, H., Möhwald, H., Mulvaney, P., Nel, A.E., Nie, S., Nordlander, P., Okano, T., Oliveira, J., Park, T.H., Penner, R.M., Prato, M., Puntes, V., Rotello, V.M., Samarakoon, A., Schaak, R.E., Shen, Y., Sjöqvist, S., Skirtach, A.G., Soliman, M.G., Stevens, M.M., Sung, H.W., Tang, B.Z., Tietze, R., Udugama, B.N., Scott VanEpps, J., Weil, T., Weiss, P.S., Willner, I., Wu, Y., Yang, L., Yue, Z., Zhang, Q., Zhang, Q., Zhang, X.E., Zhao, Y., Zhou, X., Parak, W.J., 2017. Diverse Applications of Nanomedicine. ACS Nano 11, 2313–2381. https://doi.org/10.1021/acsnano.6b06040.

Perrone, F., Craparo, E.F., Cemazar, M., Kamensek, U., Drago, S.E., Dapas, B., Scaggiante, B., Zanconati, F., Bonazza, D., Grassi, M., Truong, N., Pozzato, G., Farra, R., Cavallaro, G., Grassi, G., 2021. Targeted delivery of siRNAs against hepatocellular carcinoma-related genes by a galactosylated polyaspartamide copolymer. J. Control. Release 330, 1132–1151. https://doi.org/10.1016/j.jconrel.2020.11.020.

Puleio, R., Licciardi, M., Varvarà, P., Scialabba, C., Cassata, G., Cicero, L., Cavallaro, G., Giammona, G., 2020. Effect of actively targeted copolymer coating on solid tumors eradication by gold nanorods-induced hyperthermia. Int J Pharm 587. https://doi.org/10.1016/j.ijpharm.2020.119641.

Sanchez, L., Yi, Y., Yu, Y., 2017. Effect of partial PEGylation on particle uptake by macrophages. Nanoscale 9, 288–297. https://doi.org/10.1039/c6nr07353k.

Shaughnessy, C.A., Yadav, S., Bratcher, P.E., Zeitlin, P.L., 2022. Receptor-mediated activation of CFTR via prostaglandin signaling pathways in the airway. Am. J. Physiol. Lung Cell Mol. Physiol. 322, L305–L314. https://doi.org/10.1152/AJPLUNG.00388.2021.

Stewart, J.C.M., 1980. Colorimetric determination of phospholipids with ammonium ferrothiocyanate. Anal Biochem 104, 10–14. https://doi.org/10.1016/0003-2697(80)90269-9.

Tang, W., Perepezko, J.H., 2018. Polyamorphism and liquid-liquid transformations in D-mannitol. J. Chem. Phys. 149. https://doi.org/10.1063/1.5041757.

Triolo, D., Craparo, E.F., Porsio, B., Fiorica, C., Giammona, G., Cavallaro, G., 2017. Polymeric drug delivery micelle-like nanocarriers for pulmonary administration of beclomethasone dipropionate. Colloids Surf B Biointerfaces 151, 206–214. https://doi.org/10.1016/j.colsurfb.2016.11.025.

Zhao, Y.-Q., Li, L.-J., Zhou, E.-F., Wang, J.-Y., Wang, Y., Guo, L.-M., Zhang, X.-X., 2022. Lipid-based nanocarrier systems for drug delivery: advances and applications. Pharmaceutical Fronts 04, e43–e60. https://doi.org/10.1055/s-0042-1751036.

Zhu, Y., Liu, Y., Zhou, W., Xiang, R., Jiang, L., Huang, K., Xiao, Y., Guo, Z., Gao, J., 2010. A prostacyclin analogue, iloprost, protects from bleomycin-induced pulmonary fibrosis in mice.